Fundamentally Different Distance Dependences of Electron Transfer Rates for Low and High Driving-Forces

SCHOLARONE™
Manuscripts

Fundamentally Different Distance Dependences of Electron Transfer Rates for Low and High Driving-Forces

Svenja Neumann and Oliver S. Wenger[*]

Department of Chemistry, University of Basel, St. Johanns-Ring 19, 4056 Basel, Switzerland

Supporting Information Placeholder

ABSTRACT: The distance dependences of electron transfer rates (k_{ET}) in three homologous series of donor-bridge-acceptor compounds with reaction free energies (ΔG_{ET}^0) of ca. -1.2, -1.6, and -2.0 eV for thermal charge recombination after initial photoinduced charge-separation were studied by transient absorption spectroscopy. In the series with low driving-force, the distance dependence is normal and k_{ET} decreases upon donor-acceptor distance (r_{DA}) elongation. In the two series with higher driving-forces, k_{ET} increases with increasing distance over a certain range. This counter-intuitive behavior can be explained by a weakly distance dependent electronic donor-acceptor coupling (H_{DA}) in combination with an increasing reorganization energy (λ). Our study shows that highly exergonic electron transfers can have distance dependences that differ drastically from those of the more commonly investigated weakly exergonic reactions.

INTRODUCTION

Numerous prior studies investigated the distance dependence of electron transfer rates (k_{ET}) and the role of the intervening medium between the donor and the acceptor.[1] Rigid rod-like donor-bridge-acceptor compounds,[2-13] properly folded proteins or DNA equipped with suitable photosensitizers are particularly useful for investigations in which the donor-acceptor distance (r_{DA}) must be kept constant on the timescale of an electron transfer event.[1,14-17] Saturated hydrocarbon bridges or protein backbone typically enable long-range electron transfer via tunneling,[18,19] whereas conjugated bridges or DNA can give rise to hopping.[20-27] Though the distance dependences of k_{ET} are markedly different for these two mechanisms, both usually lead to a decrease of k_{ET} with increasing distance. Experimental studies that reported on an increase of k_{ET} at greater r_{DA} are extremely rare.[28-30] To complement such distance-dependence studies, other investigations focused on the dependence of k_{ET} on reaction free energy (ΔG_{ET}^0),[31-35] and the dependence of k_{ET} on ΔG_{ET}^0 at fixed r_{DA} is now reasonably well understood. However, we are unaware of prior systematic studies of the distance dependence of k_{ET} as a function of ΔG_{ET}^0. Against the background of our recent finding that k_{ET} can increase with increasing distance in donor-photosensitizer-acceptor triads,[36,37] and given the theoretical prediction of such counter-intuitive effects,[38,39] we explored the distance dependence of k_{ET} in the three series of triads shown in Scheme 1. These triads contain either a relatively strong triarylamine (TAA) donor with methoxy-substituents or a weaker triphenylamine (TPA) donor with chloro-substituents. As acceptors, a naphthalene diimide (NDI) unit or an anthraquinone (AQ) moiety were employed. Excitation of the metal

photosensitizers in these compounds induces rapid (≤ 10 ns) charge-separation leading to a radical pair state that subsequently undergoes thermal charge recombination between reduced acceptor and oxidized donor. The driving-force for that recombination process ($-\Delta G_{CR}^0$) varies from ca. 1.2 eV (TAA-ph$_n$-Ru-ph$_n$-NDI series) to ca. 1.6 eV (TAA-ph$_n$-Ru-ph$_n$-AQ) and ca. 2.0 eV (TPA-ph$_n$-Ir-ph$_n$-AQ). The key finding is that for the triads with $-\Delta G_{CR}^0 \approx 1.2$ eV the distance dependence of the electron transfer rate for charge recombination (k_{CR}) is normal (i. e., k_{CR} decreases with increasing distance), whereas in the two other triad series k_{CR} increases with increasing donor-acceptor separation. This shows that highly exergonic electron transfers can have distance dependences that differ fundamentally from those of the more frequently investigated weakly exergonic reactions.

Scheme 1. Structures of Molecular Triads and Driving-Forces for Charge Recombination ($-\Delta G_{CR}^0$) Between Oxidized Donors and Reduced Acceptors.
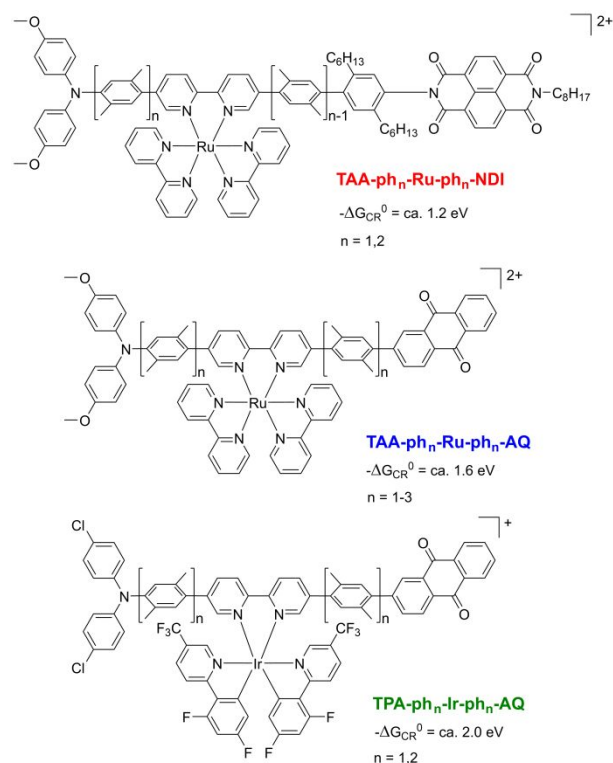

TAA-ph$_n$-Ru-ph$_n$-NDI
$-\Delta G_{CR}^0$ = ca. 1.2 eV
n = 1,2

TAA-ph$_n$-Ru-ph$_n$-AQ
$-\Delta G_{CR}^0$ = ca. 1.6 eV
n = 1-3

TPA-ph$_n$-Ir-ph$_n$-AQ
$-\Delta G_{CR}^0$ = ca. 2.0 eV
n = 1,2

Table 1. Electron Transfer Parameters for the Four New Triads: Donor-Acceptor Distance (r_{DA}), Rate Constant for Thermal Charge Recombination (k_{CR}), (Negative) Reaction Free Energy (ΔG_{CR}^0), Activation Free Energy ($\Delta G_{CR}^\ddagger$), Reorganization Energy (λ), and Electronic Donor-Acceptor Coupling (H_{DA}).

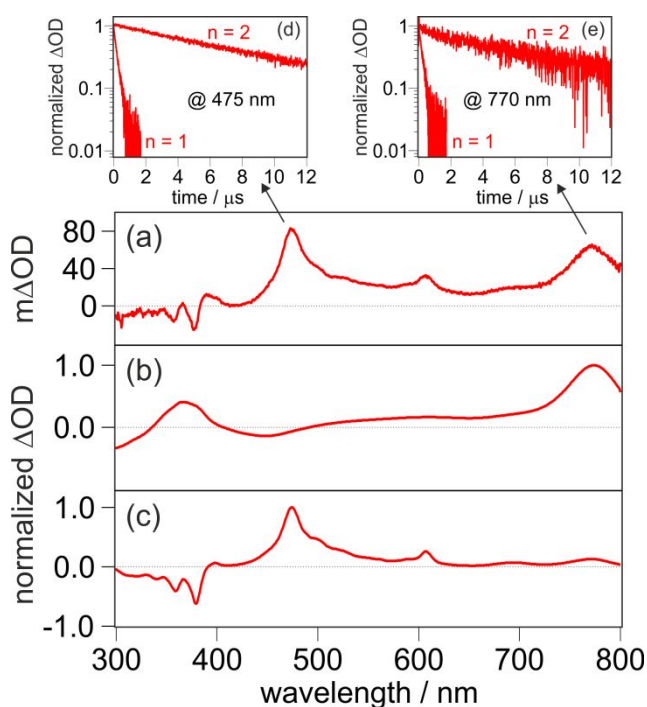| compound	r_{DA} / Å	k_{CR} / s^{-1}	$-\Delta G_{CR}^0$ / eV	$\Delta G_{CR}^\ddagger$ / meV	λ / eV	H_{DA} / cm^{-1}
TAA-ph$_1$-Ru-ph$_1$-NDI	21.7	$(4.8\pm0.5)\cdot10^6$	1.27±0.05	0	1.27±0.05	0.13±0.02
TAA-ph$_2$-Ru-ph$_2$-NDI	30.2	$(1.3\pm0.1)\cdot10^5$	1.23±0.05	47±6	1.82±0.35	0.09±0.02
TPA-ph$_1$-Ir-ph$_1$-AQ	22.0	$(1.0\pm0.1)\cdot10^6$	1.99±0.05	69±5	1.37±0.36	0.35±0.06
TPA-ph$_2$-Ir-ph$_2$-AQ	30.6	$(1.2\pm0.1)\cdot10^7$	1.96±0.05	0	1.96±0.05	0.22±0.04

Figure 1. (a) Transient UV-Vis absorption spectrum of 20 μM TAA-ph$_1$-Ru-ph$_1$-NDI in de-aerated CH$_3$CN at 20 °C. The sample was excited at 532 nm with laser pulses of ca. 10 ns duration, detection occurred by integration over a period of 200 ns immediately afterwards. (b) UV-Vis difference spectrum resulting from chemical oxidation of the TAA unit in TAA-ph$_1$-Ru-ph$_1$-NDI with Cu(ClO$_4$)$_2$ in CH$_3$CN. (c) UV-Vis difference spectrum resulting from chemical one-electron reduction of the NDI unit in TAA-ph$_1$-Ru-ph$_1$-NDI with sodium in THF. (d) Temporal evolution of the transient absorption signals for TAA-ph$_1$-Ru-ph$_1$-NDI (n = 1) and TAA-ph$_2$-Ru-ph$_2$-NDI (n = 2) monitoring the NDI$^-$ band at 475 nm. (e) Analogous to (d) but monitoring the TAA$^+$ band at 770 nm.

RESULTS AND DISCUSSION

The molecular triads were synthesized and characterized as described in the Supporting Information (SI). Cyclic voltammetry was used to determine the redox potentials of the individual components of all triads (SI page S35), leading to the $-\Delta G_{CR}^0$ values in Scheme 1. When exciting a 20 μM CH$_3$CN solution of TAA-ph$_1$-Ru-ph$_1$-NDI at 532 nm with laser pulses of ~10 ns duration, the transient absorption spectrum recorded immediately afterwards (Figure 1a) shows the spectroscopic signatures of the anticipated charge-separated state, as confirmed by the chemical oxidation and reduction UV-Vis difference spectra for TAA$^+$ (Figure 1b) and NDI$^-$ (Figure 1c). After selective excitation of the Ru(II) sensitizer at 532 nm, ^{3}MLCT-quenching by NDI followed by subsequent electron transfer from TAA to Ru(III) is mainly
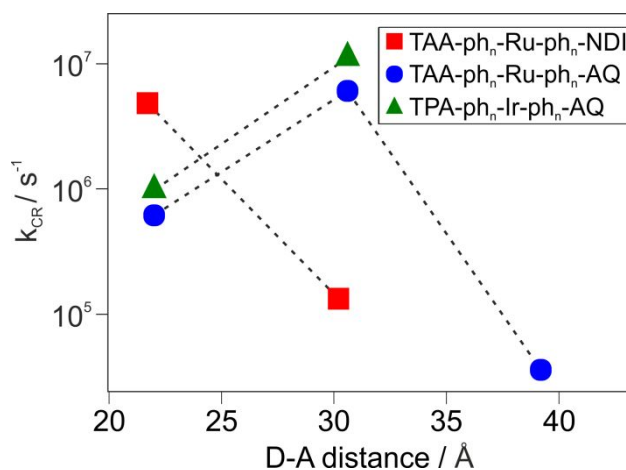

Figure 2. Distance dependence of k_{CR} in the three triad series from Scheme 1.

responsible for the rapid ($\leq$ 10 ns) formation of the observable TAA$^+$/NDI$^-$ photoproduct (SI page S41). This is also the case for the longer congener TAA-ph$_2$-Ru-ph$_2$-NDI (SI page S41). Consequently, when monitoring the temporal evolution of the TAA$^+$ and NDI$^-$ signals at the relevant wavelengths (Figure 1d/e and SI page S46), one observes instant decays due to thermal charge recombination via intra-molecular electron transfer (SI page S47). Based on kinetic measurements at 475, 607 and 770 nm, rate constants (k_{CR}) of $(4.8\pm0.5)\cdot10^6$ s^{-1} and $(1.3\pm0.1)\cdot10^5$ s^{-1} were determined for TAA-ph$_1$-Ru-ph$_1$-NDI and TAA-ph$_2$-Ru-ph$_2$-NDI in de-aerated CH$_3$CN at 20 °C (Table 1). Thus, a decrease of k_{CR} is observed when elongating r_{DA} from 21.7 to 30.2 Å (red squares in Figure 2), as commonly expected. r_{DA} corresponds to the centroid-to-centroid distances between donors and acceptors of our triads.

However, the new TAA-ph$_n$-Ru-ph$_n$-NDI data is in clear contrast to the results previously obtained for the TAA-ph$_n$-Ru-ph$_n$-AQ series of triads (Scheme 1, middle), in which the elongation from n = 1 to n = 2 caused an increase of k_{CR} by roughly a factor of 8 (blue circles in Figure 2).[36,37] In this triad series where AQ instead of NDI is the terminal acceptor, $-\Delta G_{CR}^0$ is considerably higher (ca. 1.6 eV, Scheme 1), and an activation barrier ($\Delta G_{CR}^\ddagger$) of ca. 43 meV made electron transfer in the compound with n = 1 relatively slow whilst in the triad with n = 2 it was activationless. Given the relatively strongly exergonic nature of charge recombination in that series and the expected increase of the (outer-sphere) reorganization energy (λ) with increasing distance,[40,41] these observations were attributed to a changeover from the inverted regime ($-\Delta G_{CR}^0 > \lambda$ for n = 1) to the activationless point ($-\Delta G_{CR}^0 = \lambda$ for n = 2).[36,37] This raised the question whether in a compound series with even more negative ΔG_{CR}^0 an even stronger increase of k_{CR} with increasing distance could become observable, because the reaction could be more deeply inverted in the shortest compound. This question can now

be addressed with the TPA-ph$_n$-Ir-ph$_n$-AQ series for which ΔG_{CR}^0 = ca. -2.0 eV (Scheme 1 bottom, SI page S38).

The envisioned formation of a charge-separated state storing 2.0 eV necessitated the use of a cyclometalated Ir(III) sensitizer with a photoactive ^{3}MLCT state at higher energy than that of Ru(bpy)$_3^{2+}$. In combination with a chloro-substituted triphenylamine donor and an AQ acceptor, a highly energetic charge-separated state comprised of TPA$^+$ and AQ$^-$ is indeed formed within 10 ns in both TPA-ph$_1$-Ir-ph$_1$-AQ and TPA-ph$_2$-Ir-ph$_2$-AQ after excitation at 450/420 nm (SI page S43). When monitoring the transient absorption decays at the wavelengths diagnostic for TPA$^+$ and AQ$^-$ (SI page S46), this radical ion pair is found to collapse with rate constants of $(1.0\pm0.1){\cdot}10^6$ s^{-1} in the compound with n = 1 and $(1.2\pm0.1){\cdot}10^7$ s^{-1} in the triad with n = 2 (Table 1). Evidently, electron transfer accelerates with increasing distance (green triangles in Figure 2), contrasting the behavior found for the TAA-ph$_n$-Ru-ph$_n$-NDI series (red squares in Figure 2) but in line with the TAA-ph$_n$-Ru-ph$_n$-AQ triads (blue circles in Figure 2). In the TPA-ph$_n$-Ir-ph$_n$-AQ series where charge recombination is more exergonic (ΔG_{CR}^0 = -2.0 eV), k_{CR} increases by a factor of 12 between n = 1 and n = 2, compared to a factor of 8 for the TAA-ph$_n$-Ru-ph$_n$-AQ triads (ΔG_{CR}^0 = -1.6 eV). Thus, the anticipated enhancement of the rate acceleration upon further increase of the driving-force ($-\Delta G_{CR}^0$) is indeed observable but it is modest. By measuring the charge recombination kinetics as a function of temperature (SI page S49), an activation energy of 69 meV is found for TPA-ph$_1$-Ir-ph$_1$-AQ whilst charge recombination turns out to be activationless in TPA-ph$_2$-Ir-ph$_2$-AQ (Table 1, SI page S49). Thus, in TPA-ph$_1$-Ir-ph$_1$-AQ electron transfer occurs in the more deeply inverted regime than in the previously investigated TAA-ph$_1$-Ru-ph$_1$-AQ triad ($\Delta G_{CR}^\ddagger$ = 43 meV),[36,37] as anticipated. The driving-force is essentially temperature-independent in the relevant regime (SI page S39).

It is insightful to compare all relevant electron transfer parameters in the two extreme cases of the newly investigated TAA-ph$_n$-Ru-ph$_n$-NDI and TPA-ph$_n$-Ir-ph$_n$-AQ systems (Table 1). Based on the experimentally determined activation energies, reorganization energies (λ) can be estimated (SI page S51), and they are found to increase from 1.3 - 1.4 eV in the systems with n = 1 to 1.8 - 2.0 eV in the triads with n = 2 (Table 1). The dielectric continuum model based on spherical donors and acceptors with radii of 4 Å predicts an increase in λ of ca. 0.3 eV for CH$_3$CN solvent,[36,37,40-43] but the experimentally observed effect is larger (0.5 - 0.6 eV). However, it has been noted earlier that dielectric continuum models tend to underestimate the increase of the distance-dependent outer-sphere reorganization energy (λ_0),[41] and such models cannot be expected to give an accurate quantitative description of our triads. All our compounds include a cationic photosensitizer, and the reorganization of counter-anions in the course of intramolecular electron transfer is likely to play a non-negligible role yet is not included in such models. Moreover, the experimental uncertainties in λ are up to nearly 0.4 eV (Table 1) for reasons discussed in the SI on page S51. The key point from this analysis of reorganization energies is that λ_0 shows the qualitatively expected increase upon distance elongation, but simple models are unable to provide a quantitative description of the observable effect, and large experimental uncertainties make application of more sophisticated models not worthwhile. The prior use of a model taking electron-vibrational coupling [44] into account did not lead to a significant improvement.[37]

The temperature-dependent measurements of k_{CR} furthermore give access to estimates of the electronic donor-acceptor couplings (H_{DA}, SI page S52), and we find values on the order of 0.1 – 0.4 cm^{-1} (Table 1). Depending on donor-acceptor distances and the type of molecular bridge, values in the range of 10^2 to 10^{-1} cm^{-1} are not uncommon.[45-47] The decrease in H_{DA} upon distance elongation from n = 1 to n = 2 is relatively modest and would translate to distance decay constants (β) of ca. 0.1 Å^{-1}, which is considerably lower than what is typically expected for oligo-p-phenylene bridges (β = 0.4 – 0.8 Å^{-1}).[28,47-50] However, β is not a bridge-specific parameter but instead depends on the entire combination of donor, bridge, and acceptor.[51-53] Moreover, our estimate for β can only be based on two data points, and it is possible that there are non-exponential contributions to the distance-dependent electronic coupling.[54] Evidently, our bridges all contain a bipyridine ligand and as such do not constitute a homologous series of identical elements, which is a key assumption of many models treating the distance dependence of k_{ET}.[55,56] As noted earlier,[57] distance decay constants below 0.2 Å^{-1} are likely to be an indication of a more complex situation, which may involve conformational variability and which could signal the onset of multistep hopping rather than tunneling. On the other hand, our earlier investigations of oligo-p-xylenes demonstrated that the electronic structure of this particular bridge type is significantly less length-dependent than that of oligo-p-phenylenes,[48,49,58] making a distance-dependent changeover from tunneling to hopping, such as reported previously for unsubstituted p-phenylene bridges,[28] less likely in our systems.

Using the parameters in Table 1, Marcus parabola showing k_{CR} as a function of reaction free energy (ΔG_{CR}^0) at fixed r_{DA} can be calculated (Figure 3). Upon distance elongation, the parabolas undergo the expected bottom rightward shift, due to the decrease of H_{DA} and the increase of λ with increasing distance (Table 1).[42] The driving-force is essentially constant in a given series of our triads, and this is represented by the dotted vertical lines in Figure 3. In the TAA-ph$_n$-Ru-ph$_n$-NDI series where ΔG_{CR}^0 is relatively low (-1.2 eV) this nicely visualizes the changeover from activationless electron transfer in the compound with n = 1 (red square at the top of the solid red parabola, Figure 3a) to electron transfer in the normal regime (red square in the left half of the dotted red parabola, Figure 3a) in the triad with n = 2. By contrast, in the TPA-ph$_n$-Ir-ph$_n$-AQ series, charge recombination in the compound with n = 1 occurs in the inverted regime (green triangle in the right half of the solid green parabola of Figure 3b) whilst in the compound with n = 2 it takes place at the activationless point (green triangle at the top of the dotted green parabola of Figure 3b).
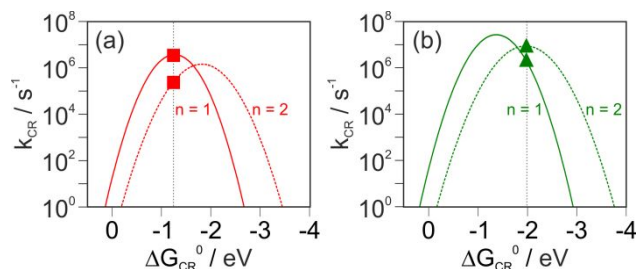

Figure 3. Plots of k_{CR} vs. ΔG_{CR}^0 based on the parameters from Table 1. (a) TAA-ph$_n$-Ru-ph$_n$-NDI systems with n = 1 (solid red) and n = 2 (dotted red). (b) TPA-ph$_n$-Ir-ph$_n$-AQ systems with n = 1 (solid green) and n = 2 (dotted green). The dotted vertical lines mark the relevant driving-forces for charge recombination.

CONCLUSIONS

In summary, our study shows that electron transfer rates can either increase or decrease with increasing donor-acceptor distance, in clear contrast to the common belief that reaction rates

always get slower when the distance between individual reactants increases.[43] This counter-intuitive behavior is readily understandable in the framework of Marcus theory, as pointed out in two early theory papers,[38,39] yet this does not seem to be nearly as widely known as the inverted driving-force effect. The present study is the first systematic investigation of the distance dependence of k_{ET} as a function of driving-force, geared at testing these early theoretical predictions. The key finding is that highly exergonic electron transfer reactions can indeed exhibit fundamentally different distance dependences than the more commonly studied weakly exergonic reactions.

The semiclassical Marcus model used herein (and in the early theoretical prediction)[38] provides an adequate qualitative description, but there is evidence from our investigations that an accurate quantitative description will require more sophisticated models.[36] Specifically, the model used herein yields relatively large increases of the outer-sphere reorganization energy paired with rather shallow distance dependences of H_{DA}. The combination of these two effects might point at a systematic error made when using the simple Marcus model.

The qualitative picture has now become fairly clear from the investigation of the 7 triads presented herein, and the simple Marcus model is very valuable to understand the little-known effect of increasing reaction rates with increasing distance. Just like the much better known inverted driving-force effect,[46,59] the phenomenon predicted by Sutin and Tachiya,[38,39] and then first observed in unambiguous manner by us,[36] might have important implications for solar energy conversion.[42] In particular, the competition between photoinduced charge-separation and (undesired) thermal charge recombination reactions in solar energy conversion devices could crucially depend on the different distance dependences of weakly and more strongly exergonic electron transfer reactions.

ASSOCIATED CONTENT

Supporting Information

Synthetic protocols and characterization data, description of equipment and methods, supplementary electrochemical and spectroscopic data, and thermochemical discussion.

AUTHOR INFORMATION

Corresponding Author

*oliver.wenger@unibas.ch

ACKNOWLEDGMENT

REFERENCES

(1) Edwards, P. P.; Gray, H. B.; Lodge, M. T. J.; Williams, R. J. P. Electron Transfer and Electronic Conduction through an Intervening Medium. *Angew. Chem. Int. Ed.* **2008**, *47*, 6758-6765.

(2) Meylemans, H. A.; Hewitt, J. T.; Abdelhaq, M.; Vallett, P. J.; Damrauer, N. H. Exploiting Conformational Dynamics to Facilitate Formation and Trapping of Electron-Transfer Photoproducts in Metal Complexes. *J. Am. Chem. Soc.* **2010**, *132*, 11464-11466.

(3) Johansson, P. G.; Kopecky, A.; Galoppini, E.; Meyer, G. J. Distance Dependent Electron Transfer at TiO_2 Interfaces Sensitized with Phenylene Ethynylene Bridged Ru^{II}-Isothiocyanate Compounds. *J. Am. Chem. Soc.* **2013**, *135*, 8331-8341.

(4) Majewski, M. B.; de Tacconi, N. R.; MacDonnell, F. M.; Wolf, M. O. Long-Lived, Directional Photoinduced Charge Separation in Ru^{II} Complexes Bearing Laminate Polypyridyl Ligands. *Chem.-Eur. J.* **2013**, *19*, 8331-8341.

(5) Sukegawa, J.; Schubert, C.; Zhu, X. Z.; Tsuji, H.; Guldi, D. M.; Nakamura, E. Electron Transfer Through Rigid Organic Molecular Wires Enhanced by Electronic and Electron-Vibration Coupling. *Nat. Chem.* **2014**, *6*, 899-905.

(6) Lee, S.-H.; Chan, C. T.-L.; Wong, K. M.-C.; Lam, W. H.; Kwok, W.-M.; Yam, V. W. W. Design and Synthesis of Bipyridine Platinum(II) Bisalkynyl Fullerene Donor–Chromophore–Acceptor Triads with Ultrafast Charge Separation. *J. Am. Chem. Soc.* **2014**, *136*, 10041-10052.

(7) Klein, J. H.; Schmidt, D.; Steiner, U. E.; Lambert, C. Complete Monitoring of Coherent and Incoherent Spin Flip Domains in the Recombination of Charge-Separated States of Donor-Iridium Complex-Acceptor Triads. *J. Am. Chem. Soc.* **2015**, *137*, 11011-11021.

(8) Hu, K.; Blair, A. D.; Piechota, E. J.; Schauer, P. A.; Sampaio, R. N.; Parlane, F. G. L.; Meyer, G. J.; Berlinguette, C. P. Kinetic Pathway for Interfacial Electron Transfer from a Semiconductor to a Molecule. *Nat. Chem.* **2016**, *8*, 853-859.

(9) Favereau, L.; Makhal, A.; Pellegrin, Y.; Blart, E.; Petersson, J.; Goransson, E.; Hammarström, L.; Odobel, F. A Molecular Tetrad That Generates a High-Energy Charge-Separated State by Mimicking the Photosynthetic Z-Scheme. *J. Am. Chem. Soc.* **2016**, *138*, 3752-60.

(10) Delor, M.; Archer, S. A.; Keane, T.; Meijer, A.; Sazanovich, I. V.; Greetham, G. M.; Towrie, M.; Weinstein, J. A. Directing the Path of Light-Induced Electron Transfer at a Molecular Fork using Vibrational Excitation. *Nat. Chem.* **2017**, *9*, 1099-1104.

(11) Schroot, R.; Schlotthauer, T.; Dietzek, B.; Jäger, M.; Schubert, U. S. Extending Long-Lived Charge Separation Between Donor and Acceptor Blocks in Novel Copolymer Architectures Featuring a Sensitizer Core. *Chem.-Eur. J.* **2017**, *23*, 16484-16490.

(12) Arrigo, A.; Santoro, A.; Puntoriero, F.; Lainé, P. P.; Campagna, S. Photoinduced Electron Transfer in Donor-Bridge-Acceptor Assemblies: The Case of Os(II)-bis(terpyridine)-(bi)pyridinium Dyads. *Coord. Chem. Rev.* **2015**, *304*, 109-116.

(13) Bao, D. D.; Upadhyayula, S.; Larsen, J. M.; Xia, B.; Georgieva, B.; Nunez, V.; Espinoza, E. M.; Hartman, J. D.; Wurch, M.; Chang, A. D.; Lin, C. K.; Larkin, J.; Vasquez, K.; Beran, G. J. O.; Vullev, V. I. Dipole-Mediated Rectification of Intramolecular Photoinduced Charge Separation and Charge Recombination. *J. Am. Chem. Soc.* **2014**, *136*, 12966-12973.

(14) Giese, B.; Amaudrut, J.; Kohler, A. K.; Spormann, M.; Wessely, S. Direct Observation of Hole Transfer Through DNA by Hopping Between Adenine Bases and by Tunnelling. *Nature* **2001**, *412*, 318-320.

(15) Genereux, J. C.; Barton, J. K. Mechanisms for DNA Charge Transport. *Chem. Rev.* **2010**, *110*, 1642-1662.

(16) Minnihan, E. C.; Nocera, D. G.; Stubbe, J. Reversible, Long-Range Radical Transfer in E-coli Class Ia Ribonucleotide Reductase. *Acc. Chem. Res.* **2013**, *46*, 2524-2535.

(17) Renaud, N.; Harris, M. A.; Singh, A. P. N.; Berlin, Y. A.; Ratner, M. A.; Wasielewski, M. R.; Lewis, F. D.; Grozema, F. C. Deep-Hole Transfer Leads to Ultrafast Charge Migration in DNA Hairpins. *Nat. Chem.* **2016**, *8*, 1015-1021.

(18) Wiberg, J.; Guo, L. J.; Pettersson, K.; Nilsson, D.; Ljungdahl, T.; Mårtensson, J.; Albinsson, B. Charge Recombination versus Charge Separation in Donor-Bridge-Acceptor Systems. *J. Am. Chem. Soc.* **2007**, *129*, 155-163.

(19) Benniston, A. C.; Harriman, A. Charge on the Move: How Electron-Transfer Dynamics Depend on Molecular Conformation. *Chem. Soc. Rev.* **2006**, *35*, 169-179.

(20) Davis, W. B.; Svec, W. A.; Ratner, M. A.; Wasielewski, M. R. Molecular-Wire Behaviour in *p*-Phenylenevinylene Oligomers. *Nature* **1998**, *396*, 60-63.

(21) Vail, S. A.; Krawczuk, P. J.; Guldi, D. M.; Palkar, A.; Echegoyen, L.; Tome, J. P. C.; Fazio, M. A.; Schuster, D. I. Energy and Electron Transfer in Polyacetylene-Linked Zinc-Porphyrin-[60]Fullerene Molecular Wires. *Chem. Eur. J.* **2005**, *11*, 3375-3388.

(22) Welter, S.; Lafolet, F.; Cecchetto, E.; Vergeer, F.; De Cola, L. Energy Transfer by a Hopping Mechanism in Dinuclear Ir^{III}/Ru^{II} Complexes: A Molecular Wire? *ChemPhysChem* **2005**, *6*, 2417-2427.

(23) Montes, V. A.; Perez-Bolivar, C.; Agarwal, N.; Shinar, J.; Anzenbacher, P. Molecular-Wire Behavior of OLED Materials: Exciton Dynamics in Multichromophoric Alq_3-Oligofluorene-Pt(II) Porphyrin Triads. *J. Am. Chem. Soc.* **2006**, *128*, 12436-12438.

(24) Barlow, S.; Risko, C.; Chung, S. J.; Tucker, N. M.; Coropceanu, V.; Jones, S. C.; Levi, Z.; Brédas, J. L.; Marder, S. R. Intervalence Transitions in the Mixed-Valence Monocations of Bis(triarylamines) Linked with Vinylene and Phenylene-Vinylene Bridges. *J. Am. Chem. Soc.* **2005**, *127*, 16900-16911.

(25) Lloveras, V.; Vidal-Gancedo, J.; Figueira-Duarte, T. M.; Nierengarten, J. F.; Novoa, J. J.; Mota, F.; Ventosa, N.; Rovira, C.; Veciana, J. Tunneling versus Hopping in Mixed-Valence Oligo-*p*-phenylenevinylene Polychlorinated Bis(triphenylmethyl) Radical Anions. *J. Am. Chem. Soc.* **2011**, *133*, 5818-5833.

(26) O'Hanlon, D. C.; Cohen, B. W.; Moravec, D. B.; Dallinger, R. F.; Hopkins, M. D. Electronic, Redox, and Photophysical Consequences of Metal-for-Carbon Substitution in Oligo-Phenylene-Ethynylenes. *J. Am. Chem. Soc.* **2014**, *136*, 3127-3136.

(27) Vela, S.; Bauroth, S.; Atienza, C.; Molina-Ontoria, A.; Guldi, D. M.; Martin, N. Determining the Attenuation Factor in Molecular Wires Featuring Covalent and Noncovalent Tectons. *Angew. Chem. Int. Ed.* **2016**, *55*, 15076-15080.

(28) Weiss, E. A.; Ahrens, M. J.; Sinks, L. E.; Gusev, A. V.; Ratner, M. A.; Wasielewski, M. R. Making a Molecular Wire: Charge and Spin Transport through *para*-Phenylene Oligomers. *J. Am. Chem. Soc.* **2004**, *126*, 5577-5584.

(29) Stangel, C.; Schubert, C.; Kuhri, S.; Rotas, G.; Margraf, J. T.; Regulska, E.; Clark, T.; Torres, T.; Tagmatarchis, N.; Coutsolelos, A. G.; Guldi, D. M. Tuning the Reorganization Energy of Electron Transfer in Supramolecular Ensembles - Metalloporphyrin, Oligophenylenevinylenes, and Fullerene - and the Impact on Electron Transfer Kinetics. *Nanoscale* **2015**, *7*, 2597-2608.

(30) Luo, Y. S.; Barthelmes, K.; Wächtler, M.; Winter, A.; Schubert, U. S.; Dietzek, B. Increased Charge Separation Rates with Increasing Donor-Acceptor Distance in Molecular Triads: The Effect of Solvent Polarity. *J. Phys. Chem. C* **2017**, *121*, 9220-9229.

(31) Waskasi, M. M.; Kodis, G.; Moore, A. L.; Moore, T. A.; Gust, D.; Matyushov, D. V. Marcus Bell-Shaped Electron Transfer Kinetics Observed in an Arrhenius Plot. *J. Am. Chem. Soc.* **2016**, *138*, 9251-9257.

(32) Rosspeintner, A.; Angulo, G.; Vauthey, E. Bimolecular Photoinduced Electron Transfer Beyond the Diffusion Limit: The Rehm-Weller Experiment Revisited with Femtosecond Time Resolution. *J. Am. Chem. Soc.* **2014**, *136*, 2026-2032.

(33) Suneesh, C. V.; Balan, B.; Ozawa, H.; Nakamura, Y.; Katayama, T.; Muramatsu, M.; Nagasawa, Y.; Miyasaka, H.; Sakai, K. Mechanistic Studies of Photoinduced Intramolecular and Intermolecular Electron Transfer Processes in RuPt-centred Photo-Hydrogen-Evolving Molecular Devices. *Phys. Chem. Chem. Phys.* **2014**, *16*, 1607-1616.

(34) Lim, G. N.; Obondi, C. O.; D'Souza, F. A High-Energy Charge-Separated State of 1.70 eV from a High-Potential Donor-Acceptor Dyad: A Catalyst for Energy-Demanding Photochemical Reactions. *Angew. Chem. Int. Ed.* **2016**, *55*, 11517-11521.

(35) Higashino, T.; Yamada, T.; Yamamoto, M.; Furube, A.; Tkachenko, N. V.; Miura, T.; Kobori, Y.; Jono, R.; Yamashita, K.; Imahori, H. Remarkable Dependence of the Final Charge Separation Efficiency on the Donor-Acceptor Interaction in Photoinduced Electron Transfer. *Angew. Chem. Int. Ed.* **2016**, *55*, 629-633.

(36) Kuss-Petermann, M.; Wenger, O. S. Increasing Electron-Transfer Rates with Increasing Donor-Acceptor Distance. *Angew. Chem. Int. Ed.* **2016**, *55*, 815-819.

(37) Kuss-Petermann, M.; Wenger, O. S. Electron Transfer Rate Maxima at Large Donor-Acceptor Distances. *J. Am. Chem. Soc.* **2016**, *138*, 1349-1358.

(38) Brunschwig, B. S.; Ehrenson, S.; Sutin, N. Distance Dependence of Electron Transfer Reactions - Rate Maxima and Rapid Rates at Large Reactant Separations. *J. Am. Chem. Soc.* **1984**, *106*, 6858-6859.

(39) Tachiya, M.; Murata, S. New Explanation for the Lack of the Inverted Region in Charge Separation Reactions. *J. Phys. Chem.* **1992**, *96*, 8441-8444.

(40) Marcus, R. A.; Sutin, N. Electron Transfers in Chemistry and Biology. *Biochim. Biophys. Acta* **1985**, *811*, 265-322.

(41) Isied, S. S.; Vassilian, A.; Wishart, J. F.; Creutz, C.; Schwarz, H. A.; Sutin, N. The Distance Dependence of Intramolecular Electron-Transfer Rates - Importance of the Nuclear Factor. *J. Am. Chem. Soc.* **1988**, *110*, 635-637.

(42) Kuss-Petermann, M.; Wenger, O. S. Unusual Distance Dependences of Electron Transfer Rates. *Phys. Chem. Chem. Phys.* **2016**, *18*, 18657-18664.

(43) Kuss-Petermann, M.; Wenger, O. S. Reaction Rate Maxima at Large Distances between Reactants. *Chimia* **2016**, *70*, 177-181.

(44) Barbara, P. F.; Meyer, T. J.; Ratner, M. A. Contemporary Issues in Electron Transfer Research. *J. Phys. Chem.* **1996**, *100*, 13148-13168.

(45) Kirk, M. L.; Shultz, D. A.; Depperman, E. C.; Brannen, C. L. Donor-Acceptor Biradicals as Ground State Analogues of Photoinduced Charge Separated States. *J. Am. Chem. Soc.* **2007**, *129*, 1937-1943.

(46) Fox, L. S.; Kozik, M.; Winkler, J. R.; Gray, H. B. Gaussian Free-Energy Dependence of Electron-Transfer Rates in Iridium Complexes. *Science* **1990**, *247*, 1069-1071.

(47) Weiss, E. A.; Tauber, M. J.; Kelley, R. F.; Ahrens, M. J.; Ratner, M. A.; Wasielewski, M. R. Conformationally Gated Switching between Superexchange and Hopping within Oligo-*p*-phenylene-based Molecular Wires. *J. Am. Chem. Soc.* **2005**, *127*, 11842-11850.

(48) Hanss, D.; Wenger, O. S. Electron Tunneling through Oligo-*p*-xylene Bridges. *Inorg. Chem.* **2008**, *47*, 9081-9084.

(49) Hanss, D.; Wenger, O. S. Tunneling Barrier Effects on Photoinduced Charge Transfer through Covalent Rigid Rod-Like Bridges. *Inorg. Chem.* **2009**, *48*, 671-680.

(50) Indelli, M. T.; Chiorboli, C.; Flamigni, L.; De Cola, L.; Scandola, F. Photoinduced Electron Transfer across Oligo-*p*-phenylene Bridges. Distance and Conformational Effects in Ru(II)-Rh(III) Dyads. *Inorg. Chem.* **2007**, *46*, 5630-5641.

(51) Natali, M.; Campagna, S.; Scandola, F. Photoinduced Electron Transfer across Molecular Bridges: Electron- and Hole-Transfer Superexchange Pathways. *Chem. Soc. Rev.* **2014**, *43*, 4005-4018.

(52) Eng, M. P.; Albinsson, B. The Dependence of the Electronic Coupling on Energy Gap and Bridge Conformation Towards Prediction of the Distance Dependence of Electron Transfer Reactions. *Chem. Phys.* **2009**, *357*, 132-139.

(53) Lewis, F. D.; Liu, J. Q.; Weigel, W.; Rettig, W.; Kurnikov, I. V.; Beratan, D. N. Donor-Bridge-Acceptor Energetics Determine the Distance Dependence of Electron Tunneling in DNA. *Proc. Natl. Acad. Sci. U. S. A.* **2002**, *99*, 12536-12541.

(54) Eng, M. P.; Albinsson, B. Non-Exponential Distance Dependence of Bridge-Mediated Electronic Coupling. *Angew. Chem. Int. Ed.* **2006**, *45*, 5626-5629.

(55) McConnell, H. M. Intramolecular Charge Transfer In Aromatic Free Radicals. *J. Chem. Phys.* **1961**, *35*, 508-515.

(56) Wenger, O. S. How Donor-Bridge-Acceptor Energetics Influence Electron Tunneling Dynamics and Their Distance Dependences. *Acc. Chem. Res.* **2011**, *44*, 25-35.

(57) Berlin, Y. A.; Grozema, F. C.; Siebbeles, L. D. A.; Ratner, M. A. Charge Transfer in Donor-Bridge-Acceptor Systems: Static Disorder, Dynamic Fluctuations, and Complex Kinetics. *J. Phys. Chem. C* **2008**, *112*, 10988-11000.

(58) Hanss, D.; Walther, M. E.; Wenger, O. S. Importance of Covalence, Conformational Effects and Tunneling-barrier Heights for Long-range Electron Transfer: Insights from Dyads with Oligo-*p*-phenylene, Oligo-*p*-xylene and Oligo-*p*-dimethoxybenzene Bridges. *Coord. Chem. Rev.* **2010**, *254*, 2584-2592.

(59) Closs, G. L.; Miller, J. R. Intramolecular Long-distance Electron-transfer in Organic Molecules. *Science* **1988**, *240*, 440-447.

Electron transfer rates usually decrease with increasing donor-acceptor distance. However, at very high driving-forces opposite behavior is observable. The synthesis and characterization of two new sets of molecular triads allowed us to perform systematic studies on the distance dependence of electron transfer rates with a particular focus on the influence of driving-forces.